The Effects of Carrier-Velocity Saturation on High-Current BJT Output Resistance

Sang-Gug Lee and Robert M. Fox, *Member, IEEE*

Abstract—**Modern Bipolar Junction Transistors (BJT's) tend to operate with saturated carrier velocity in the collector space-charge region. This paper presents a physical analysis of the effects of velocity saturation on the output resistance of BJT's, especially for high current levels. Physical analyses show that when the collector current density approaches a critical value, the Early voltage can increase significantly due to carrier-velocity saturation as the resulting base push-out partially offsets base-width modulation. This effect is also demonstrated in simulations with PISCES and MMSPICE.**

I. Introduction

ANALOG circuits such as operational amplifiers typically employ active loads to achieve high gains. The voltage gain and frequency response of such circuits thus depend on the transistors' small-signal output resistance. In most contemporary bipolar junction transistors (BJT's), high electric fields occur in the collector junction space-charge region due to the high epilayer doping or high reverse-bias voltage. These high fields tend to saturate the free-electron drift velocity.

This work is a study of the effects of carrier-velocity saturation, especially for high current levels, on the output resistance characteristics of BJT's. Analytical expressions for normalized BJT output resistance are derived for an idealized structure as an aid to qualitative understanding. MMSPICE [1] and PISCES-II [2] simulations are also provided.

II. Analysis

In a recent letter, Roulston [3] presented an improved model for the Early voltage V_A in n-p-n transistors with very narrow base widths (less than 0.1 μm). Roulston concluded that, due to carrier-velocity saturation, a substantial improvement in Early voltage is expected in narrow-base transistors compared to estimates based only on the base doping level and width. Liou's [4] correction to this work led to the following:

$$V_A = V_{A0}[1 + D_n F_c / v_s W_{B0}] \quad (1)$$

Manuscript received October 16, 1990; revised May 17, 1991. This work was supported by the Semiconductor Research Corporation under Contract 89-SP-087. The review of this paper was arranged by Associate Editor D. D. Tang.

The authors are with the Department of Electrical Engineering, University of Florida, Gainesville, FL 32611.

IEEE Log Number 9105346.

where $V_{A0} = W_{B0}/(dW_{B0}/dV_{CE})$ is the conventional expression for Early voltage (neglecting velocity saturation), D_n is the electron diffusion constant, F_c is an empirical factor to account for built-in fields and bandgap narrowing in the base region, v_s is the electron saturation velocity, and W_{B0} is the quasi-neutral base width. For a silicon bipolar transistor with a base width of 0.04 μm, $D_n = 17\ \text{cm}^2/\text{V} \cdot \text{s}$, and $F_c = 1$, this model predicts $V_A = 1.4V_{A0}$.

With carrier-velocity saturation the carrier concentration in the space-charge region (SCR) is proportional to the collector current, and the positions of the SCR boundaries become functions of the carrier concentration. Roulston's model accounts only for a reduction in the concentration gradient due to the nonzero carrier concentration at the SCR boundary. From (1), this leads to significant increase in V_A only for very narrow base widths. As is well known, at the level of collector current where the SCR boundaries become strong functions of J_C, base-width modulation due to increments in V_{CB} tends to be offset by base push-out (Kirk effect) [5] as the resulting increase in n_c (and J_c) redistributes the electric fields in the SCR. This offsetting mechanism, which was neglected in [3], can lead to a much more significant increase in small-signal output resistance at high currents, even for ordinary base widths.

Following is a derivation of this increase in output resistance as represented by the Early voltage. The Early voltage [6] can be considered as the output resistance normalized by the collector current: $V_A = r_o I_C - V_{CE}$ where r_o is the output resistance and I_C is the collector current. To simplify the mathematics, base and buried-layer dopings are assumed constant, and the buried-layer doping is assumed much greater than the base doping, which is much greater than epidoping. The base terminal is assumed to be driven by a constant voltage source (Fig. 1) and the emitter junction SCR width is assumed to be independent of the collector current. The base–collector bias voltage and the resulting electric field are assumed to be high enough to saturate the electron velocity even near the SCR edge. By this assumption we are excluding the possibility of ohmic quasi-saturation even though, in practice, the transistor might enter that operating region at low V_{CB}. Ohmic quasi-saturation is excluded from this analysis since it can be treated without considering velocity saturation.

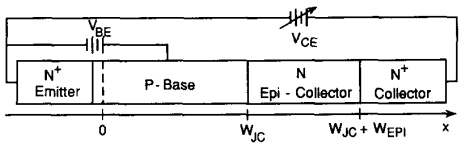

Fig. 1. One-dimensional n-p-n transistor structure.

Three operating conditions are considered: (Case 1) forward-active with part of the epitaxial layer quasi-neutral, (Case 2) forward-active with the epilayer entirely space-charged, and (Case 3) nonohmic quasi-saturation [7].

A. Case 1

Fig. 2(a) shows the electron concentration and electric field distribution for the case of forward-active operation with part of the epilayer quasi-neutral (QN). In the SCR, the current flows predominantly by drift. Assuming velocity saturation, the collector current density J_C can be expressed as

$$J_C = qn_c v_s \tag{2}$$

where n_c is the electron concentration in the SCR required to support the current. Equation (2) and the equality of charges on both sides of the collector junction lead to the relation

$$x_B(qN_A + J_C/v_s) = x_C(qN_{\text{EPI}} - J_C/v_s) \tag{3}$$

where x_B is the penetration of the SCR into the base, x_C is the penetration of the SCR into the epilayer, N_{EPI} is the epilayer doping concentration, and N_A is the base doping concentration. Poisson's equation can be solved in the collector junction SCR to yield the following expression:

$$V_{CB} + \phi_C = \frac{1}{2\epsilon_s}\left[\left(qN_A + \frac{J_C}{v_s}\right)x_B^2 + \left(qN_{\text{EPI}} - \frac{J_C}{v_s}\right)x_C^2\right] \tag{4}$$

where V_{CB} is the collector junction reverse bias, ϕ_C is the collector junction built-in potential, and ϵ_s is the semiconductor permittivity. In (4) the potential drop across the QN portion of the epilayer is neglected for simplicity. The effect of this approximation on output resistance will be discussed later. From (3) and (4), x_B can be written in terms of V_{CB} and J_C as

$$x_B = \sqrt{\frac{2\epsilon_s N_{\text{EPI}}(V_{CB} + \phi_C)}{qN_A(N_{\text{EPI}} + N_A)}}\sqrt{\frac{1 - J_C/J_{\text{EPI}}}{1 + J_C/J_A}} = x_{B0}\sqrt{\frac{1 - J_C/J_{\text{EPI}}}{1 + J_C/J_A}} \tag{5}$$

where

$$x_{B0} = \sqrt{\frac{2\epsilon_s N_{\text{EPI}}(V_{CB} + \phi_C)}{qN_A(N_{\text{EPI}} + N_A)}} \tag{6}$$

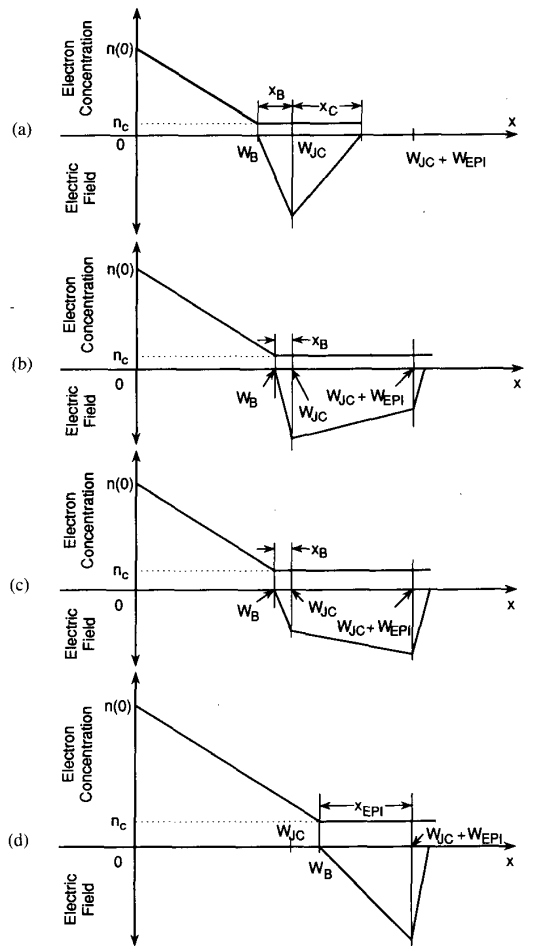

Fig. 2. Typical electron concentration and electric field distribution for (a) forward-active operation with part of the epitaxial layer quasi-neutral; (b) forward-active operation with the epilayer entirely space-charged, $J_C < J_{\text{EPI}}$; (c) forward-active operation with the epilayer entirely space-charged, $J_C > J_{\text{EPI}}$; (d) nonohmic quasi-saturation operation.

$J_{\text{EPI}} = qN_{\text{EPI}}v_s$, and $J_A = qN_A v_s$. x_{B0} is the SCR penetration into the base which would result from neglecting velocity saturation (i.e., using the depletion approximation).

Fig. 3 shows a plot of x_B/x_{B0} as a function of collector current density J_C. The QN base width (W_B) with carrier-velocity saturation can be expressed by

$$W_B = W_{JC} - x_B \tag{7}$$

while the base width neglecting velocity saturation (W_{B0}) is expressed by

$$W_{B0} = W_{JC} - x_{B0}. \tag{8}$$

As can be seen from Fig. 3, as J_C approaches J_{EPI}, x_B decreases rapidly. Therefore, dW_B/dV_{CE} differs significantly from the value dW_{B0}/dV_{CE} found in Roulston [3, eq. (1)].

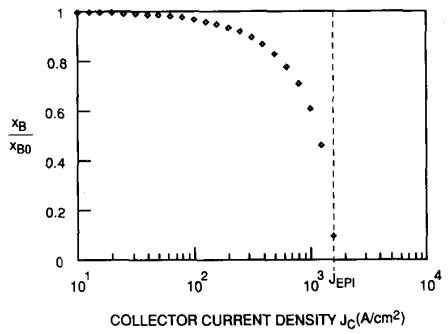

Fig. 3. Plot of the ratio x_B/x_{B0} as a function of collector current density J_C for $N_A = 1 \times 10^{17}$ cm^{-3} and $N_{EPI} = 1 \times 10^{15}$ cm^{-3}.

J_C can be expressed as

$$J_C = \kappa q D_n [n(0) - n_c]/W_B \tag{9}$$

where κ is an empirical factor that allows for drift current and $n(0)$ is the electron concentration at the edge of emitter-base SCR in the base region (Fig. 2(a)). Using (2), (9), and the definition of the Early voltage, V_A can be expressed as

$$V_A = -[W_B + \kappa D_n/v_s](dV_{CE}/dW_B). \tag{10}$$

Therefore, from (5), (7), and (10), we obtain

$$V_A \cong \frac{W_B(V_{CB} + \phi_C)}{0.5x_B}\left[1 + \frac{\kappa D_n}{v_s W_B} + \frac{\epsilon_s v_s (V_{CB} + \phi_C) J_C}{x_B W_B (J_C + J_A)^2}\right]. \tag{11}$$

Similarly, an expression for the Early voltage neglecting velocity saturation can be found from (8)–(10), assuming $n_c = 0$, as

$$V_{A0} \cong \frac{W_{B0}(V_{CB} + \phi_C)}{0.5x_{B0}}. \tag{12}$$

Equation (11) is similar in form to (1) except for the addition of a third term in the brackets. The last two terms have only a small effect on V_A except for very narrow base widths. For $J_C > 0.1J_{EPI}$, however, (11) predicts more significant increases in V_A due to the $(1 - J_C/J_{EPI})^{1/2}$ dependence of x_B in the factor $W_B(V_{CB} + \phi_C)/(0.5x_B)$ in (11).

Equation (11) is valid only up to the value of J_C for which the base-collector SCR extends all the way to the buried layer for a given value of V_{CB}, i.e., when $x_C = W_{EPI}$. The upper limit of validity for (11) can be found from (3) and (5) with x_C replaced by W_{EPI}

$$J_C|_{x_C = W_{EPI}} \cong \frac{J_{EPI}}{1 + \frac{N_A}{N_{EPI}}\left(\frac{x_{B0}}{W_{EPI}}\right)^2}\left[1 - \left(\frac{x_{C0}}{W_{EPI}}\right)^2\right] \tag{13}$$

where

$$x_{C0} = \sqrt{\frac{2\epsilon_s N_A (V_{CB} + \phi_C)}{qN_{EPI}(N_{EPI} + N_A)}} \tag{14}$$

is the value of x_C obtained from the depletion approximation. For typical BJT's, $(N_A/N_{EPI})\,(x_{B0}/W_{EPI})^2 << 1$. Thus when $W_{EPI} >> x_{C0}$, (11) is valid for values of J_C very close to J_{EPI}, so that the effect of carrier-velocity saturation on V_A can be very large.

B. Case 2

As J_C increases above $J_C|_{x_C = W_{EPI}}$ the collector–base SCR begins to uncover charge in the buried layer. The resulting electron concentration and electric field distribution are shown in Fig. 2(b). As the current increases above J_{EPI}, the electron concentration in the epi rises above N_{EPI}, leading to field and electron concentration distributions as shown in Fig. 2(c). Using charge neutrality and solving Poisson's equation over the collector junction SCR, x_B for Case 2 (Fig. 2(b) and (c)) can be written as

$$x_B \cong -W_{EPI} + \sqrt{W_{EPI}^2\left[1 + \frac{N_{EPI}(1 - J_C/J_{EPI})}{N_A(1 + J_C/J_A)}\right] + \frac{2\epsilon_s(V_{CB} + \phi_C)}{qN_A(1 + J_C/J_A)}}. \tag{15}$$

From (7), (10), and (15), the Early voltage V_A can be expressed as

$$V_A \cong \frac{qN_A}{2\epsilon_s}\left(1 + \frac{J_C}{J_A}\right)\left\{2\left(W_B + \frac{\kappa D_n}{v_s}\right)(W_{EPI} + x_B) + \frac{J_C/J_A}{(1 + J_C/J_A)^2}\left[W_{EPI}^2 + \frac{2\epsilon_s(V_{CB} + \phi_C)}{qN_A}\right]\right\}. \tag{16}$$

C. Case 3

Further increments in J_C drive the BJT into nonohmic quasi-saturation (NOQS). Fig. 2(d) shows a typical electron concentration and electric field distribution in NOQS. In NOQS operation, the epi-SCR excess free-electron concentration $(n_c - N_{EPI})$ is balanced by the heavily doped buried-layer charge. Solution of Poisson's equation leads to

$$x_{EPI} \cong \sqrt{\frac{2\epsilon_s(V_{CB} + \phi_C)}{qN_{EPI}(J_C/J_{EPI} - 1)}} \tag{17}$$

whre x_{EPI} is the epilayer SCR width in NOQS operation (Fig. 2(d)). In this case W_B must be redefined as

$$W_B = W_{JC} + W_{EPI} - x_{EPI}. \tag{18}$$

Combining this expression with (10) and (18) yields an Early voltage expression for NOQS mode

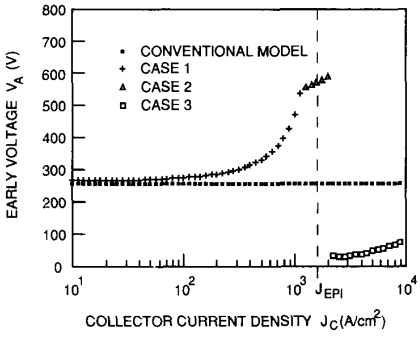

Fig. 4. Comparison of conventional and improved V_A models for a transistor with $N_A = 1 \times 10^{17}$ cm^{-3}, $N_{EPI} = 1 \times 10^{15}$ cm^{-3}, $W_{JC} = 0.5$ μm, $W_{EPI} = 7$ μm, and $V_{CB} = 10$ V as a function of J_C.

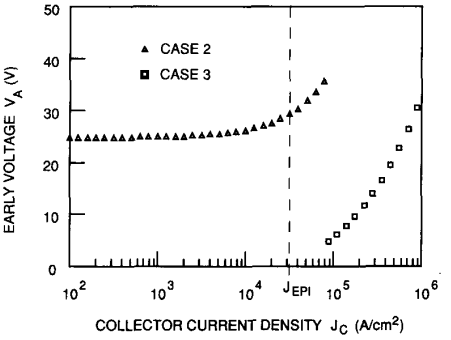

Fig. 5. Plot of the improved V_A model for a transistor with $N_A = 0.5 \times 10^{18}$ cm^{-3}, $N_{EPI} = 1 \times 10^{16}$ cm^{-3}, $W_{JC} = 0.1$ μm, $W_{EPI} = 0.35$ μm, and $V_{CB} = 3$ V. The epilayer is depleted completely even at low current.

$$V_A = \frac{W_B(V_{CB} + \phi_C)}{0.5x_{EPI}} \cdot \left[1 + \frac{\kappa D_n}{v_s W_B} + \frac{\epsilon_s v_s (V_{CB} + \phi_C) J_C}{x_{EPI} W_B (J_C - J_{EPI})^2}\right]. \quad (19)$$

The upper limit of validity for (16) and the lower limit for (19) can be found by replacing x_{EPI} with W_{EPI} in (17)

$$J_C|_{x_{EPI} = W_{EPI}} \cong J_{EPI}[1 + (x_{C0}/W_{EPI})^2]. \quad (20)$$

Fig. 4 shows a plot of the Early voltage using (11), (16), and (19) and using the "conventional" analysis (12) assuming $\kappa = 1$ and $D_n = 17$ cm^2/V · s. In (11), (16), and (19), κ is usually greater than 1, especially for high currents, but this has only a small effect on the resulting Early voltage.

In Fig. 4, discrepancies between the conventional and improved moels at low currents are as Roulston predicted. The dependence of the SCR boundary position on electron concentration has little effect on low currents. However, for J_C greater than about $0.1J_{EPI}$, this effect becomes significant and V_A increases rapidly as J_C approaches J_{EPI} until the entire epilayer becomes space-charged (Case 1). As mentioned earlier, the potential drop across the QN epi is neglected in (11). At low currents this drop is negligible. As the current approaches J_{EPI}, the IR drop becomes more significant, increasing V_A slightly more than predicted by (11). However, the resistance of the QN epi itself drops with increasing current due to the reduced width of QN epi. Thus V_A should again be as predicted by (11) at the boundary between Cases 1 and 2, where the QN epi width reaches zero.

For J_C greater than $J_C|_{x_C = W_{EPI}}$ (Case 2), the Early voltage continues to increase, but at a slower rate than in Case 1. In this case, the heavier buried-layer doping reduces the rate of base push-out with increasing J_C.

As can be seen in the figure, V_A drops at the transition between Cases 2 and 3 as the device enters nonohmic quasi-saturation. As shown, V_A can even drop below the prediction of the conventional model. For $J_C >> J_{EPI}$, V_A becomes proportional to $(J_C)^{1/2}$.

For very high base-collector reverse biases or very narrow epi-thicknesses the epilayer can become completely depleted even at low currents. For this case (11) is not valid, and (16) is valid for any current up to the value of J_C given by (20). Equation (19) remains valid for NOQS operation. Fig. 5 shows the Early voltage variation as a function of J_C for $\kappa = 1$, $D_n = 17$ cm^2/V · s, and $V_{CB} = 3$ V for a BJT with a 0.35-μm epi-thickness, which is thin enough to allow epilayer depletion at low currents. As shown in the figure, carrier-velocity saturation can still enhance the output resistance considerably in forward-active mode for $J_C > J_{EPI}$.

III. Numerical Simulations

A series of numerical simulations were performed using PISCES-II and MMSPICE to verify that these effects can indeed occur. In PISCES-II the effect of carrier-velocity saturation on Early voltage was studied by performing simulations with and without the field-dependent mobility which models carrier-velocity saturation. Several BJT structures were simulated, and the results were consistent with analysis. Fig. 6 shows a comparison of V_A behavior with and without field-dependnet mobility for a transistor with a 1.9-μm-thick epilayer. As can be seen in Fig. 6, using the field-dependent mobility model, V_A does increase considerably at high currents, whereas with the field-dependent mobility turned off, V_A increases only slightly (due to emitter-side base-width modulation). In the lower curve (with field-dependent mobility turned off) the Early voltage drops at high currents. This effect can be explained by the onset of ohmic quasi-saturation.

The physics-based BJT model in the circuit simulator MMSPICE [1] includes a charge-based model for advanced high-speed transistors based on one-dimensional analysis of carrier transport. The analysis accounts for high-current effects and impact ionization. The model covers all of the cases considered in the above analyses. Appropriate charge equations are applied to the various regions of the device, allowing for moving regional boundaries. The resulting set of coupled equations require iterative numerical solution. The highly physical basis of this approach allows the software to be used for device simulation as well as for circuit simulation.

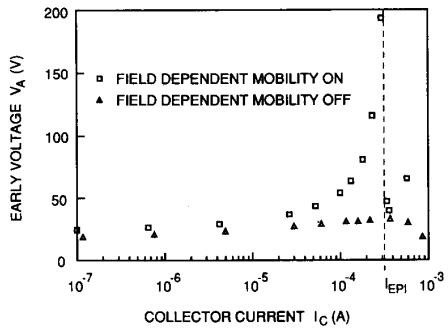

Fig. 6. PISCES-II simulation of Early voltage variation as a function of collector current. The device was similar to MOSAIC III BJT [8] except the epi was extended to 1.9 μm. $N_{EPI} = 1 \times 10^{16}$ cm^{-3}, $W_{JC} \cong 0.15$ μm, and $V_{CB} = 10$ V.

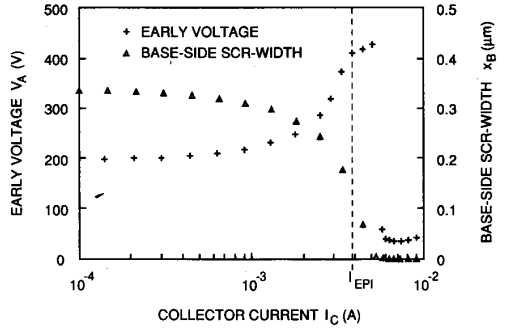

Fig. 7. MMSPICE simulation results of Early voltage and SCR penetration into the base as a function of collector current for a typical analog BJT with $N_{EPI} = 1 \times 10^{15}$ cm^{-3}, base width $\cong 0.8$ μm, epi-width $\cong 7$ μm, and $V_{CB} = 15$ V.

We have modified MMSPICE to allow output of internal physical parameters (e.g., x_B, x_C, QN base width, and QN epi-width), in addition to the usual voltage and current outputs. Fig. 7 shows V_A and x_B variations for a typical analog BJT as a function of I_C for a fixed V_{CE}. As can be seen in the figure, MMSPICE predicts substantial increases in Early voltage due to carrier-velocity saturation at high currents. Fig. 7 also clearly shows that the Early voltage enhancements are associated with variations in x_B.

IV. Conclusions

The analysis in Section II demonstrates that BJT output resistance can be raised significantly by carrier-velocity saturation. For typical base widths, there are usually small increases in output resistance at low currents, but the most important effects are predicted for currents close to the critical value J_{EPI}. These effects are also predicted by PISCES and by the highly physical circuit/device simulator MMSPICE. In practice, thermal feedback tends to severely degrade the output resistance at high currents [9]–[11] which tends to mask the V_A enhancement. With an operating point chosen near J_{EPI} it may be possible to design high-speed, high-power amplifiers with very high voltage gain if operation is restricted to frequencies high enough to avoid thermal feedback.

References

[1] H. Jeong, "MMSPICE: A physical alternative to Gummel-Poon/SPICE and a semi-numerical mixed-mode simulator for advanced bipolar technology CAD," Ph.D. dissertation, University of Florida, Gainesville, Dec. 1989.

[2] M. R. Pinto, C. S. Rafferty, H. R. Yeager, and R. W. Dutton, "PISCES-IIB User's Manual and Supplement Report," Stanford Electronics Lab. Tech. Rep., Stanford Univ., Stanford, CA, 1985.

[3] D. J. Roulston, "Early voltage in very-narrow-base bipolar transistors," *IEEE Electron Device Lett.*, vol. 11, pp. 88–89, 1990.

[4] J. J. Liou, "Comments on 'Early voltage in very-narrow-base transistors'," *IEEE Electron Device Lett.*, vol. 11, no. 5, p. 236, May 1990.

[5] C. T. Kirk, Jr., "A theory of transistor cutoff frequency (f_t) fall-off at high current densities," *IRE Trans. Electron Devices*, vol. ED-9, p. 164, 1962.

[6] I. E. Getreu, *Modeling the Bipolar Transistor.* New York: Elsevier, 1978, p. 226.

[7] H. Jeong and J. G. Fossum, "A charge-based large-signal bipolar transistor model for device and circuit simulation," *IEEE Trans. Electron Devices*, vol. 36, no. 1, pp. 124–131, Jan. 1989.

[8] P. J. Zdebel, R. J. Balda, B.-Y. Hwang, V. d.t. Torre, and A. Wagner, "MOSAIC III—A high performance bipolar technology with advanced self-aligned devices," in *IEEE Bipolar Circuits and Technology Meet.*, 1987, pp. 172–175.

[9] O. Muller, "Internal thermal feedback in four-poles especially in transistors," *Proc. IEEE*, vol. 52, pp. 924–930, Aug. 1964.

[10] G. Meijer, "The current dependency of the output conductance of voltage-driven bipolar transistors," *IEEE J. Solid-State Circuits*, vol. SC-12, no. 4, pp. 428–429, Aug. 1977.

[11] R. M. Fox and S.-G. Lee, "Predictive modeling of thermal effects in BJTs," in *IEEE Bipolar Circuits and Technology Meet.*, Oct. 1991.

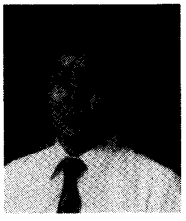

Sang-Gug Lee was born in KyungNam, Korea, in 1958. He received the B.S. degree in electronic engineering from KyungPook National University, TaeGu, Korea, in 1981, and the M.E. degree in electrical engineering from University of Florida, Gainesville, in 1989. He is currently working toward the Ph.D. degree at University of Florida, specializing in BJT small-signal modeling.

From 1983 to 1986, he was an Instructor in the Department of Electronic Engineering at the Naval Academy, JinHae, Korea.

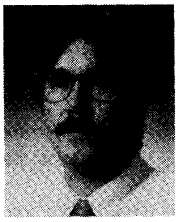

Robert M. Fox (S'78–M'80) was born in Birmingham, AL, on November 12, 1950. He received the B.S. degree in physics from the University of Notre Dame, Notre Dame, IN, in 1972, and the M.S. and Ph.D. degrees in electrical engineering from Auburn University, Auburn, AL, in 1981 and 1986, respectively.

Since 1986, he has served as Assistant Professor of Electrical Engineering at the University of Florida, Gainesville. His research interests center on circuit design for advanced silicon technologies.

Dr. Fox is a member of the Audio Engineering Society, ASEE, Phi Kappa Phi, and Eta Kappa Nu.